Supporting Information

Enhanced Nitrate-to-Ammonia Conversion through Ag-Cu-P Catalyst for Sustainable Ammonia Generation under Ambient Conditions

Xinwei Wen[a], Yue Zhao[a], Puyang Fan[a], Jiajie Wu[a], Kai Xiong[c], Chang Liu[a], Qing Qu[a*] and Lei Li[b*]

[a] School of Chemical Science and Technology, Yunnan University, Kunming 650091, China

[b] State Key Laboratory for Conservation and Utilization of Bio-Resources in Yunnan, Yunnan University, Kunming 650091, China

c School of Materials and Energy, Yunnan University, Kunming 650091, China

*Corresponding author: Qing Qu; quqing@ynu.edu.cn

Supporting Figures and Tables

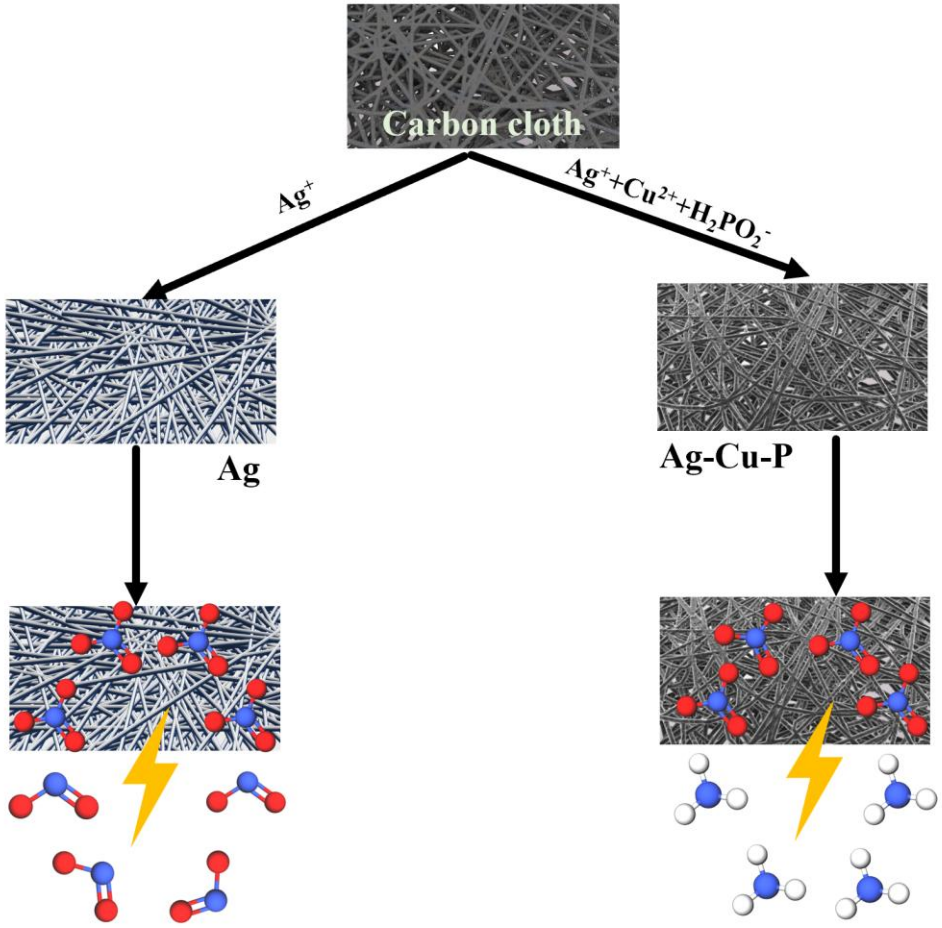

Figure S1. The synthetic route of Ag/CP and Ag-Cu-P/CP.

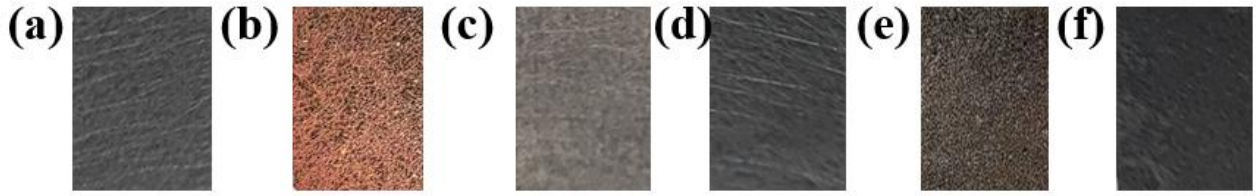

Figure S2. The digital pictures of blank carbon paper (a), Cu coating/CP (b), Ag coating/CP (c), nano-Ag/CP (d), Ag-Cu/CP (e), and Ag-Cu-P/CP (f).

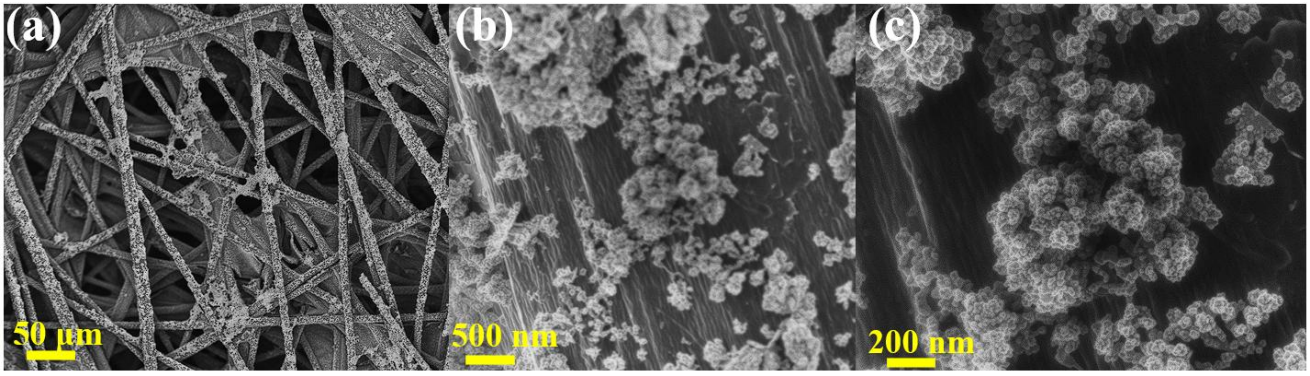

Figure S3. The SEM images of nano Ag/CP.

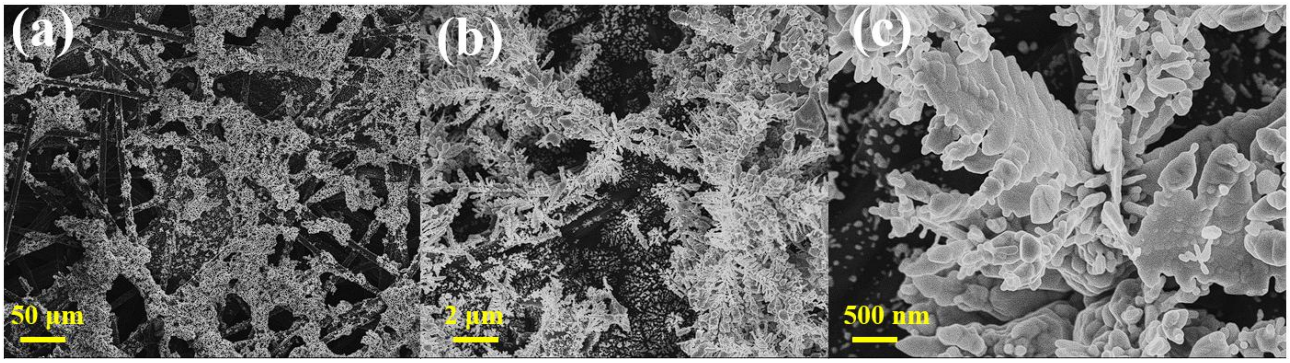

Figure S4. The SEM images of Ag coating/CP.

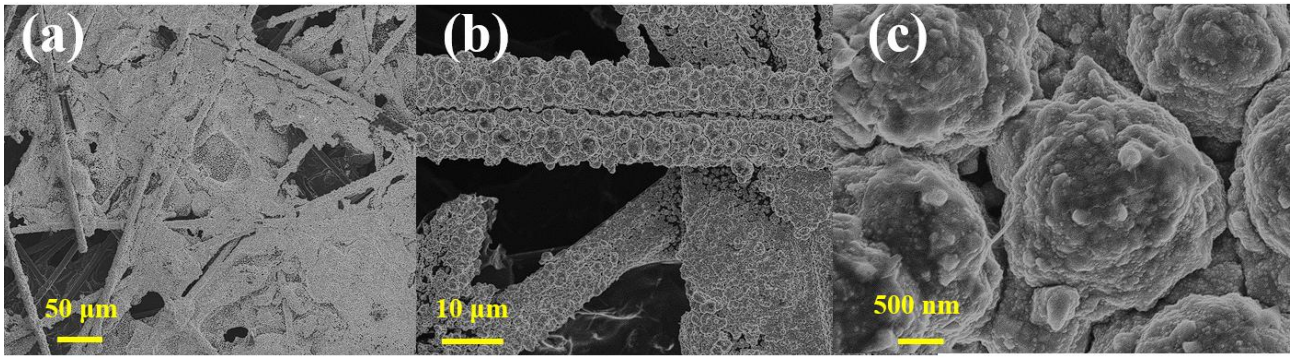

Figure S5. The SEM images of Cu coating/CP.

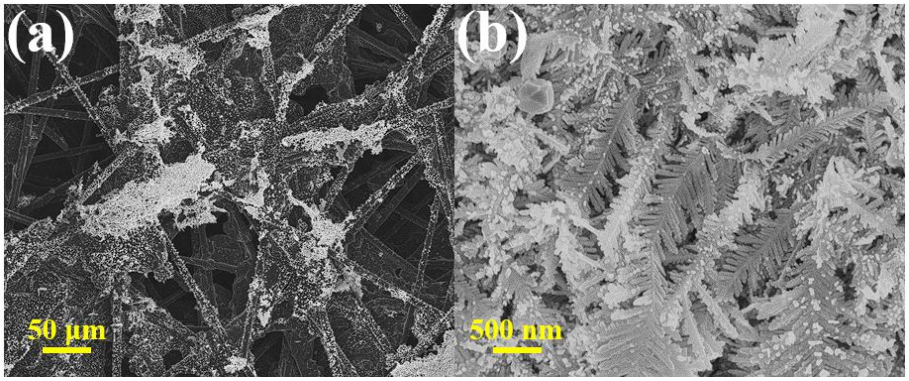

Figure S6. The SEM images of Ag-Cu/CP.

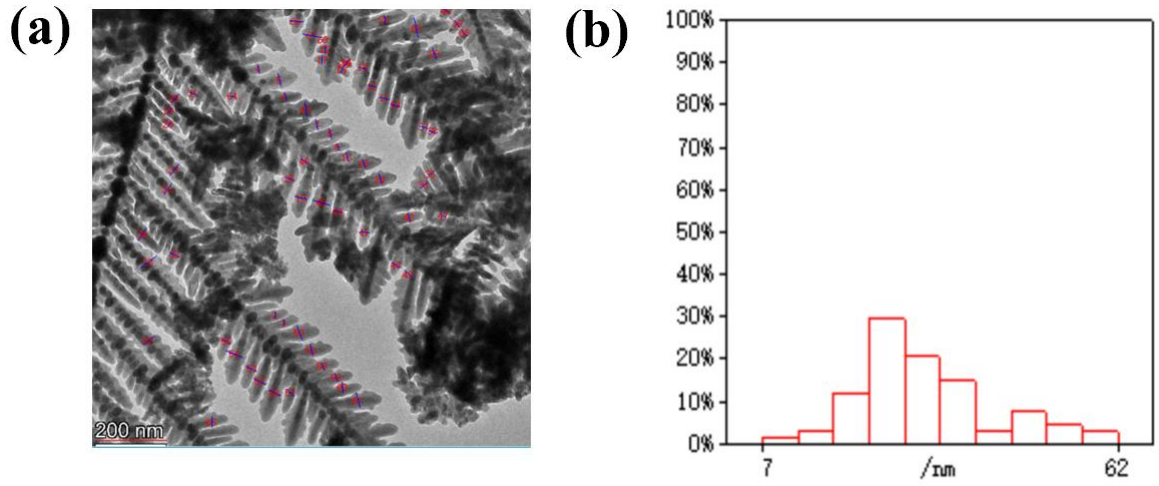

Figure S7. The particle size statistics of Ag-Cu-P.

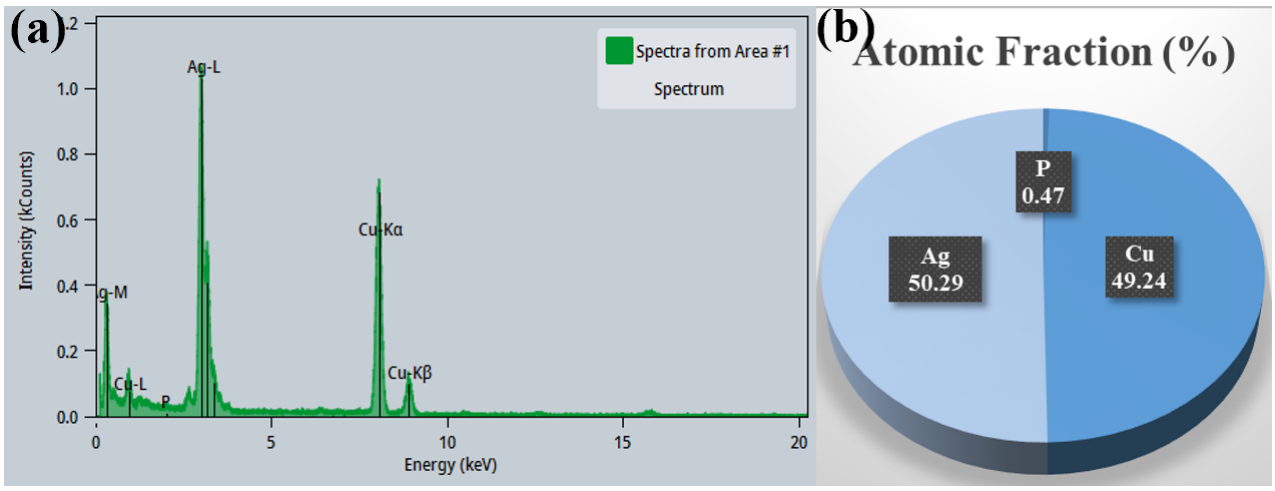

Figure S8. Elemental Scale Diagram of Ag-Cu-P (a), (b).

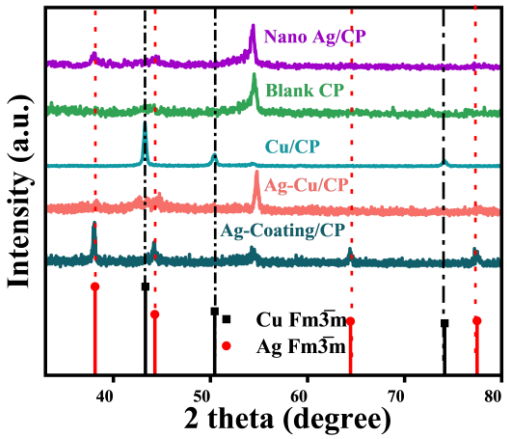

Figure S9. The XRD pattern of nano Ag/CP, blank carbon paper, Cu coating/CP, Ag-Cu/CP, and Ag coating/CP.

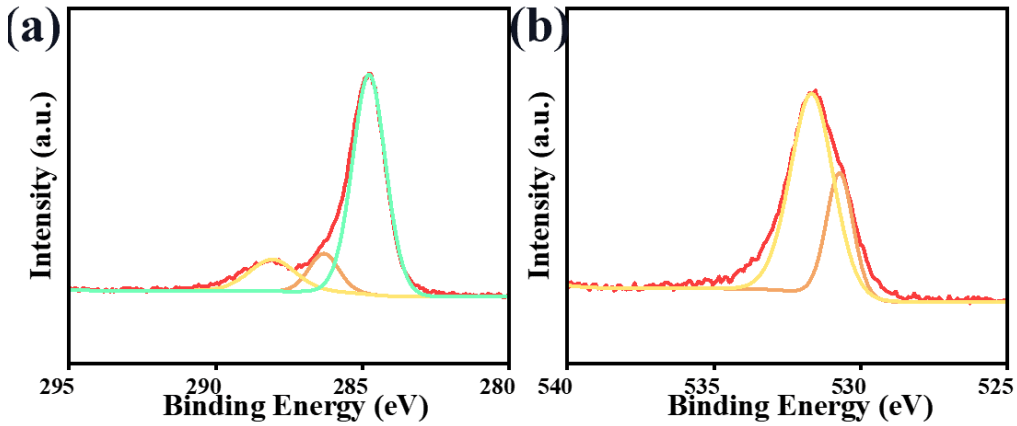

Figure S10. **The O (a) and C (b) XPS spectra of Ag-Cu-P.**

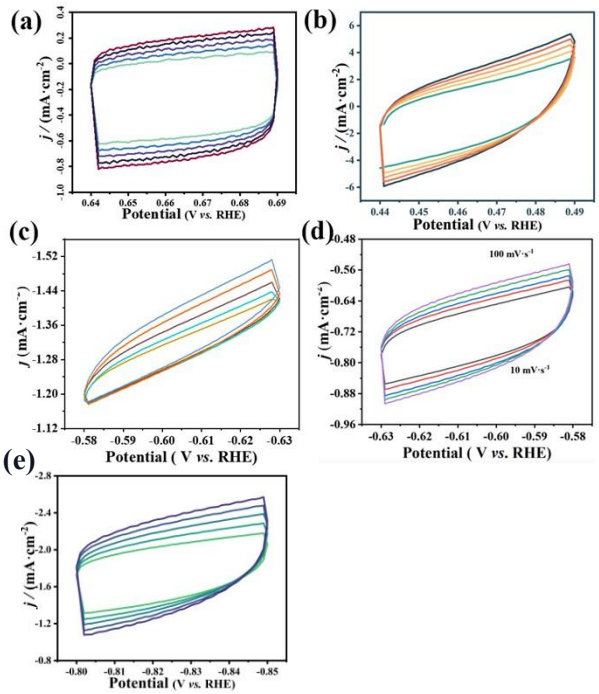

Figure S11. Typical CV curves of catalysts Ag coating/CP (a), Ag-Cu-P/CP (b), nano Ag/CP (c), blank CP (d), and Ag-Cu/CP.

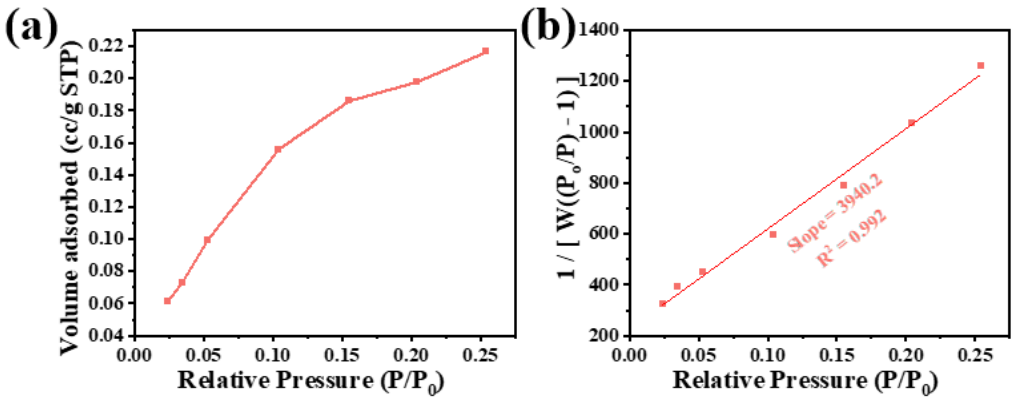

Figure 12. Isotherms (a) and fitting curves (b) of carbon paper

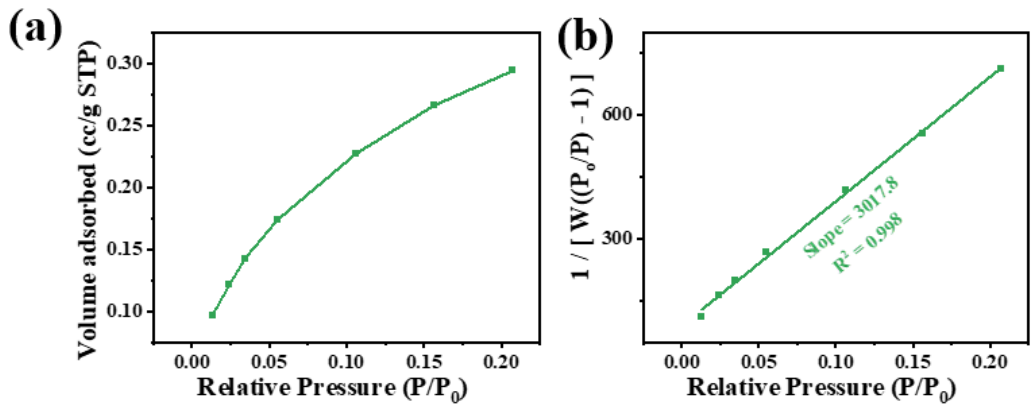

Figure 13. Isotherms (a) and fitting curves (b) of Ag-Cu-P/CP.

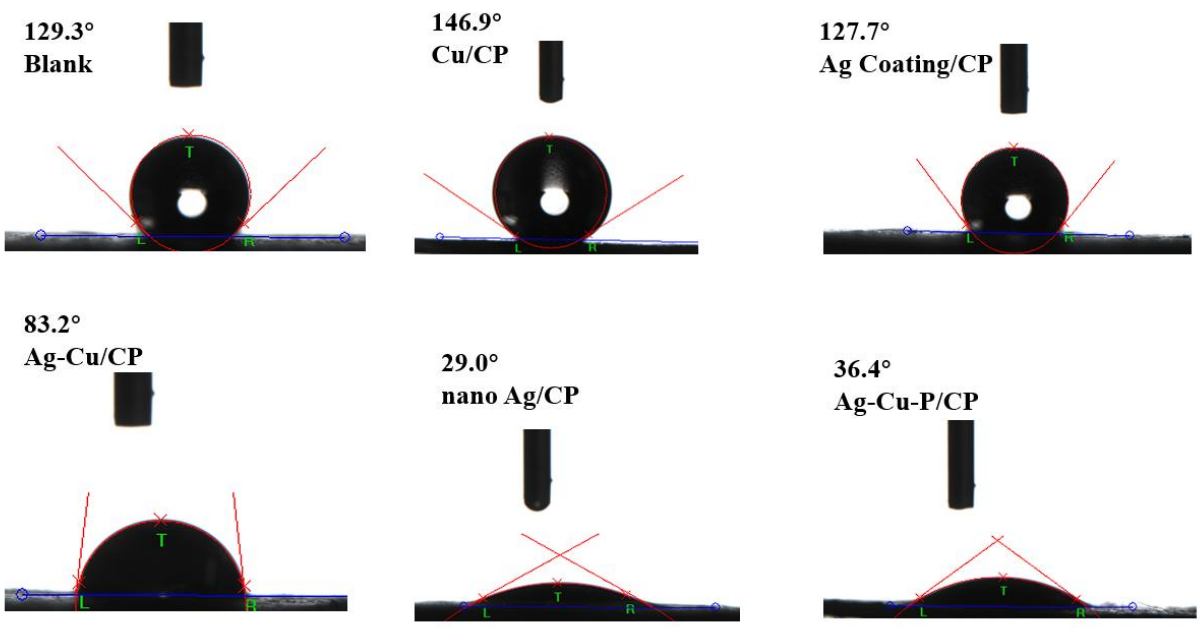

Figure S14. The Contact Angle Measurements on different catalyst's surface.

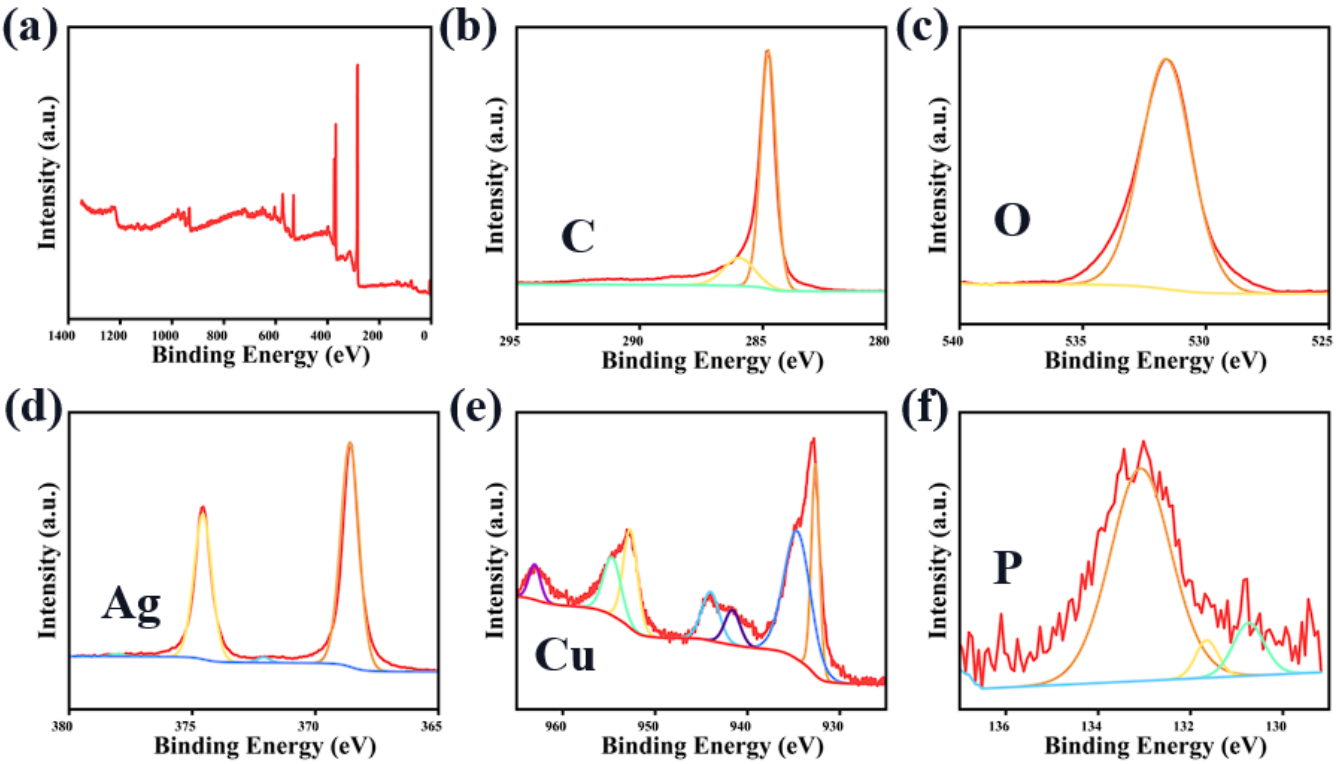

Figure S15. **The XPS spectra of Ag-Cu-P (a), C 1s (b), O 1s (c), Ag 3d (d), Cu 2p (e), and P 3p (f) after stability test.**

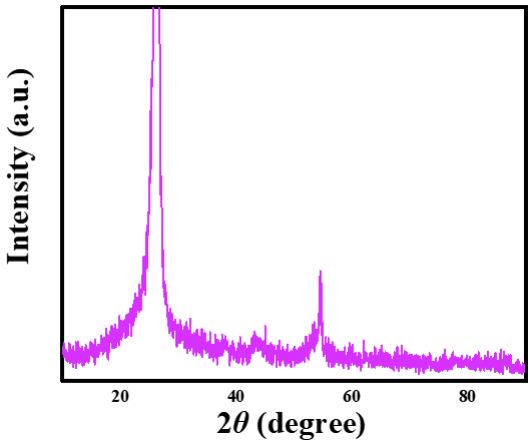

Figure S16. The XRD pattern of Ag-Cu-P after stability test.

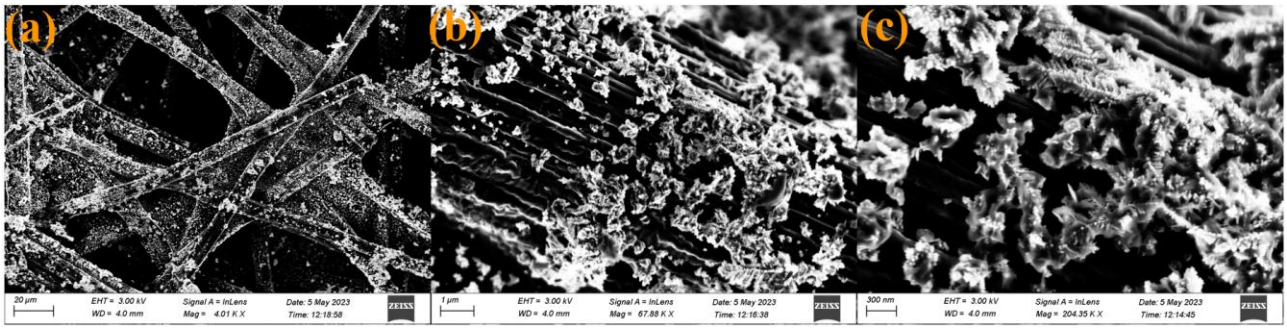

Figure S17. The SEM images of Ag-Cu-P/CP after the stability test.

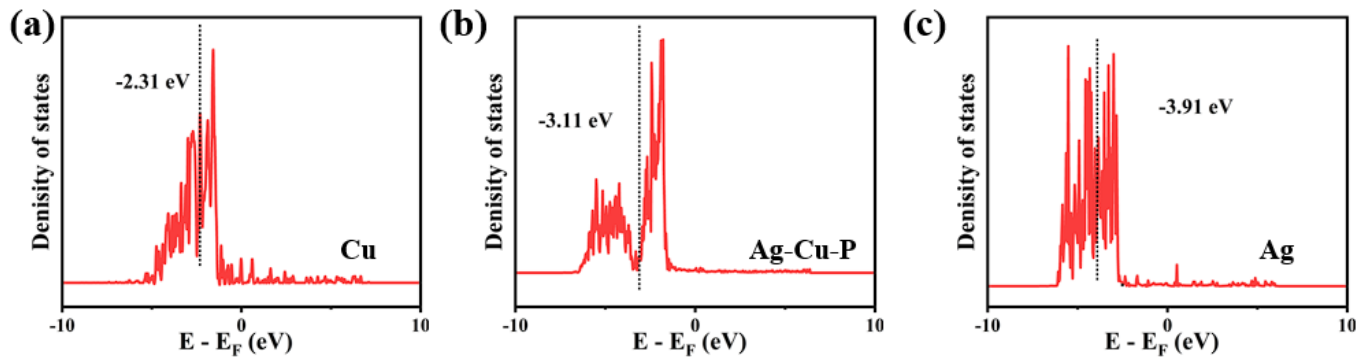

Figure S18. The PDOS plot of Cu, Ag-Cu-P, and Ag.

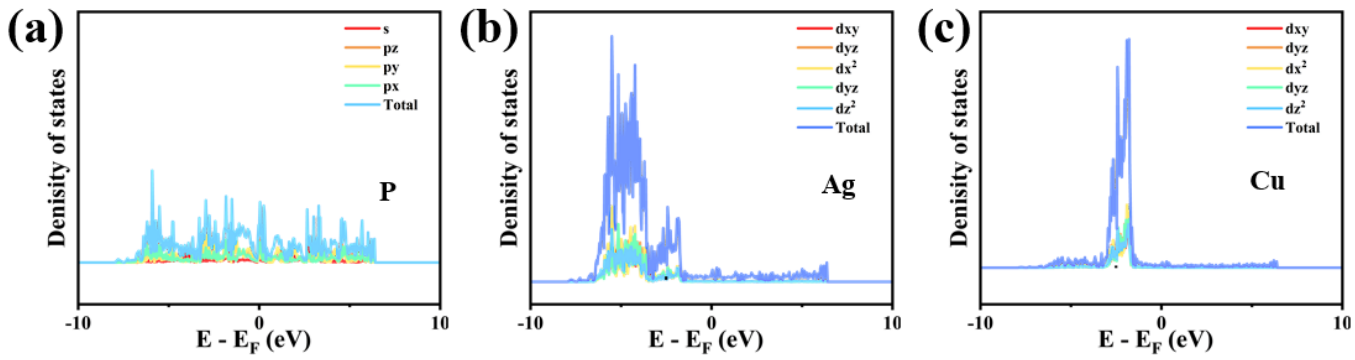

Figure S19. Calculated PDOS of Ag-Cu-P.

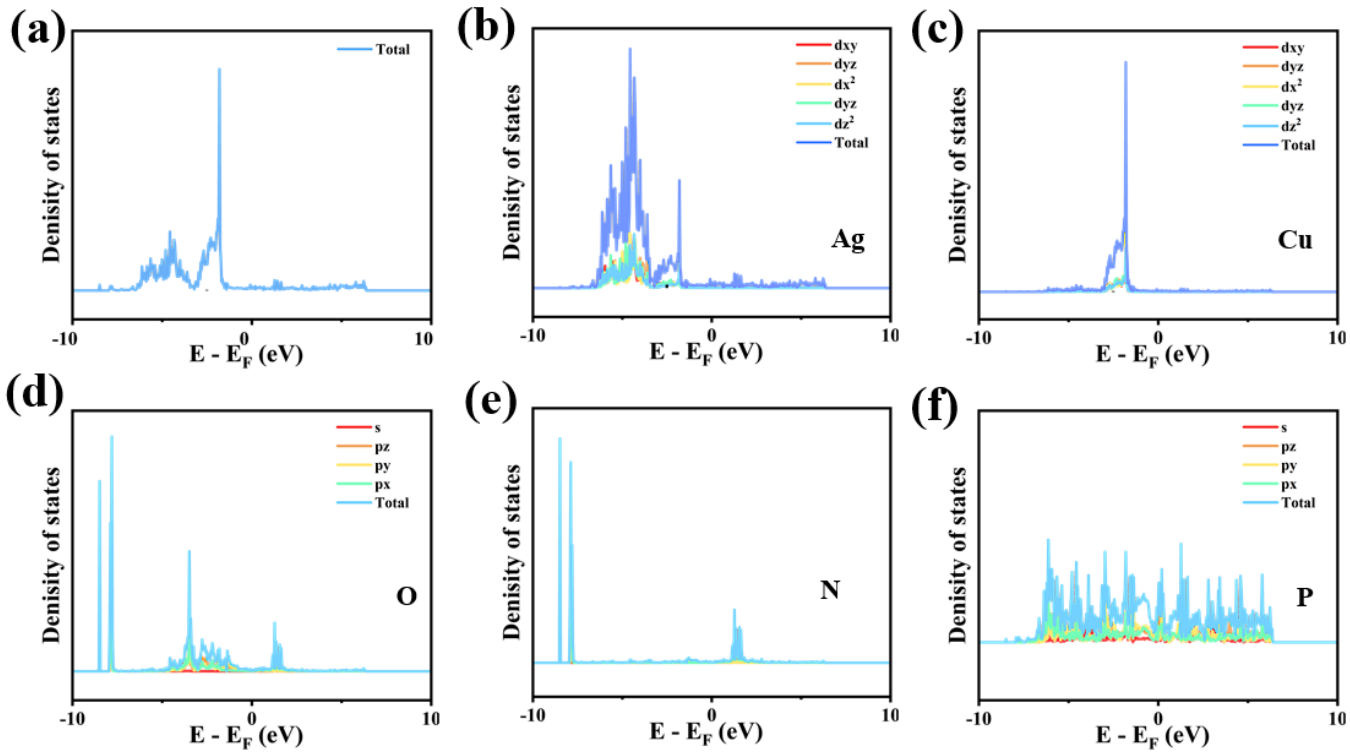

Figure S20. Calculated PDOS of *NO_3 on (111) surface of Ag-Cu-P.

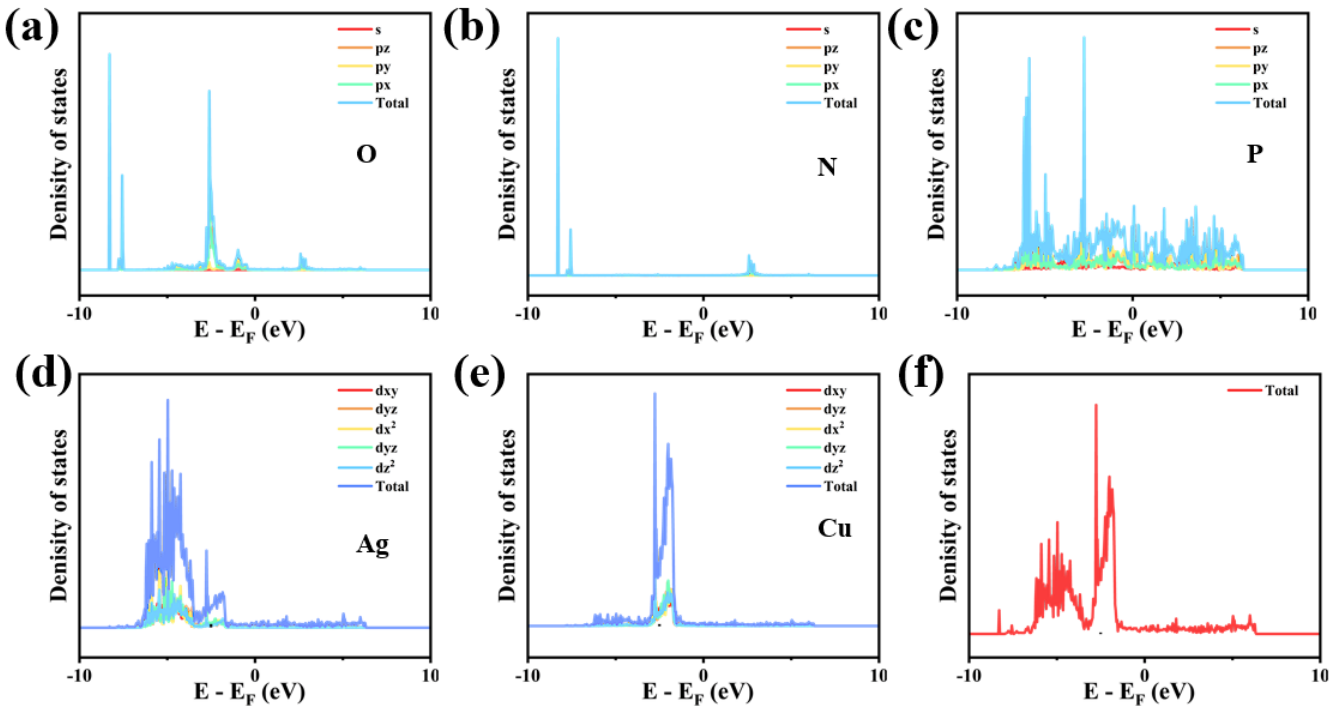

Figure S21. Calculated PDOS of *NO_2 on (111) surface of Ag-Cu-P.

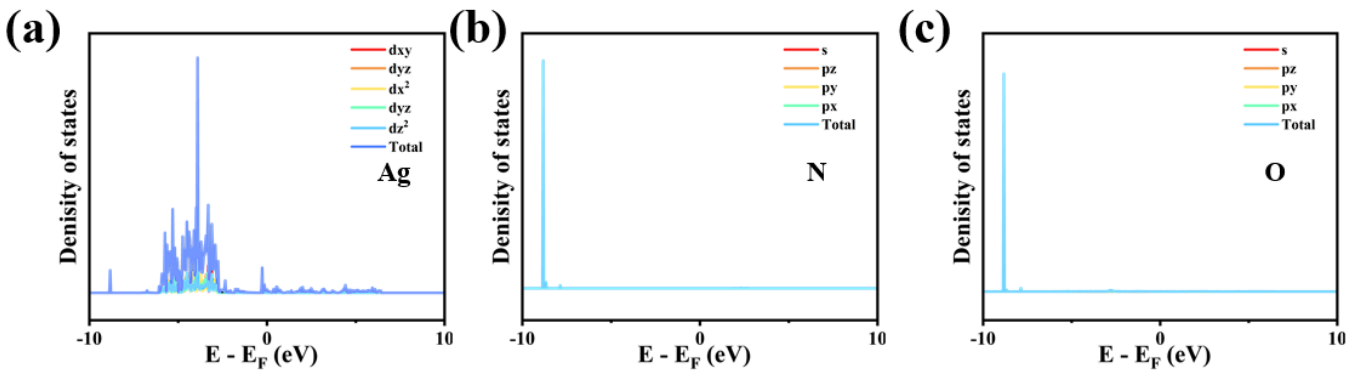

Figure S22. Calculated PDOS of *NO_3 on (111) surface of Ag.

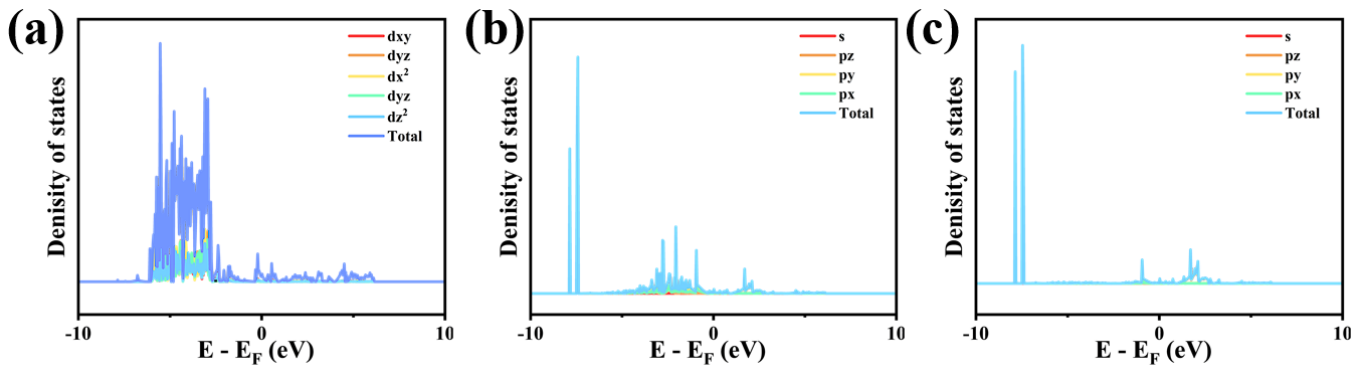

Figure S23. Calculated PDOS of *NO_2 on (111) surface of Ag.

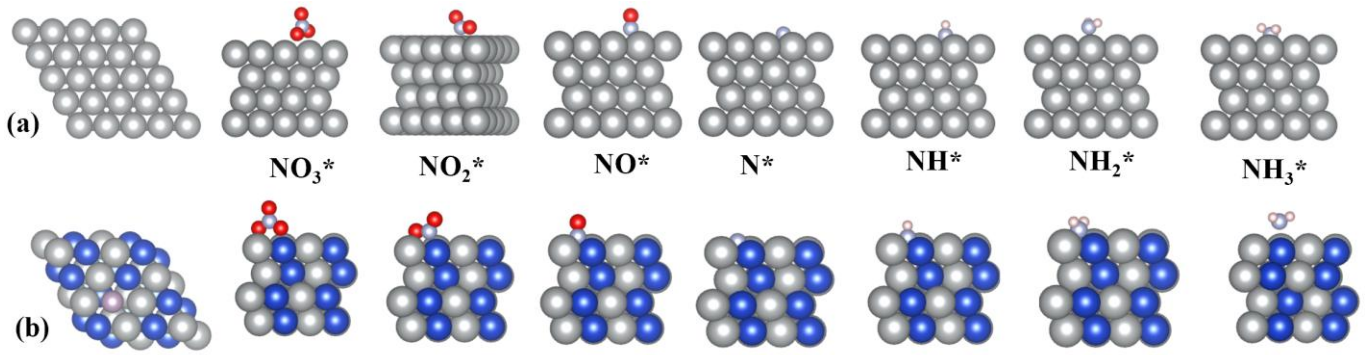

Figure S24. The adsorption configurations in the NO_3RR process of Ag (a) and Ag-Cu-P (b).

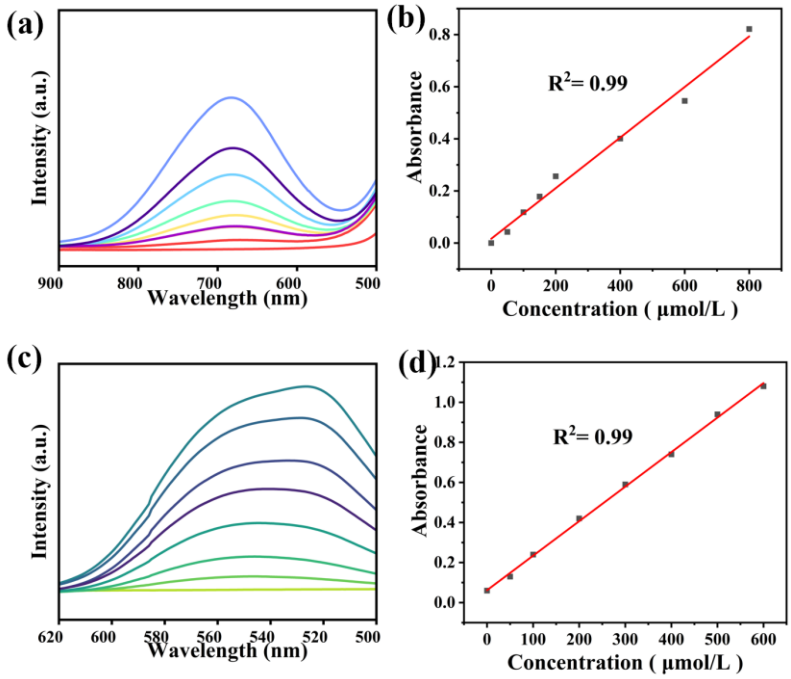

Figure S25. The UV-visible absorption spectra and corresponding fitting curves for various concentrations of NH_4^+ (a), (b), and NO_2^- (c), (d).

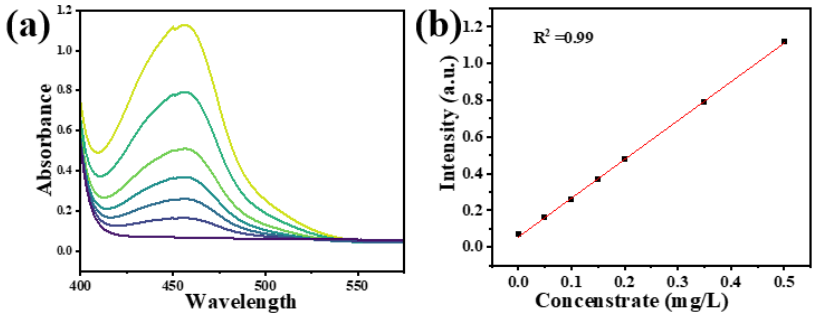

Figure S26. The UV-visible absorption spectra and corresponding fitting curves for various concentrations of N_2H_4 (a), and (b).

Table S1. The elemental composition of Ag-Cu-P.

Element	Family	Atomic Fraction (%)	Atomic Error (%)	Mass Fraction (%)	Mass Error (%)
P	K	0.47	0.05	0.17	0.02
Cu	K	49.24	4.57	36.52	4.25
Ag	L	50.29	4.56	63.31	4.25

Table S2. The C_{dl} and ECSA of different catalysts.

Catalysts	C_{dl} (mF)	ECSA (cm^{-2})
Carbon Paper	0.28	/
Ag coating/CP	0.33	8.25
nano Ag/CP	1.05	26.25
Cu coating/CP	2.39	59.75
Ag-Cu/CP	1.90	47.50
Ag-Cu-P/CP	7.41	185.25

Table S3. BET analysis data for Ag-Cu-P/CC.

Relative Pressure	Volume	1 / [W((P$_o$/P) - 1)]	Summary
1.31E-02	0.0967	1.10E+02	
2.42E-02	0.1215	1.64E+02	Slope = 3017.8 g^{-1}
3.43E-02	0.1427	1.99E+02	Intercept = 89.6 g^{-1}
5.51E-02	0.1736	2.69E+02	R^2 = 0.999
1.06E-01	0.2274	4.18E+02	Surface Area =1.12 m^2/g
1.56E-01	0.2661	5.57E+02	
2.07E-01	0.2942	7.11E+02	

Table S4. BET analysis data for carbon paper

Relative Pressure	Volume	1 / [W((P$_o$/P) - 1)]	Relative Pressure
2.40E-02	0.0611	3.22E+02	
3.47E-02	0.0732	3.92E+02	Slope = 3940.2 g^{-1}
5.29E-02	0.0995	4.50E+02	Intercept = 225.4 g^{-1}
1.04E-01	0.156	5.96E+02	R^2 = 0.999
1.55E-01	0.186	7.89E+02	Surface Area =0.836 m^2/g
2.04E-01	0.1978	1.04E+03	
2.54E-01	0.2165	1.26E+03	

Table S5. The Rs and R_{ct} of different catalysts

Catalysts	R_s	R_{ct}
Carbon Paper	4.3	/
Ag coating/CP	2.2	19.3
nano Ag/CP	2.3	9.6
Cu coating/CP	3.3	12.6
Ag-Cu/CP	2.3	12.7
Ag-Cu-P/CP	1.7	3.2

Table S6. The potentional at 10 mA/cm^2 of different catalysts in different reactions.

Catalysts	NO_3RR (mV)	NO_2RR (mV)
Ag-Cu-P/CP	256	-9
nano Ag/CP	241	-139
Ag-Cu/CP	231	-184
Ag coating/CP	228	-239
Cu coating/CP	102	-176

Table S7. Calculated Gibbs free energies of Ag at different pH.

△G	pH=14	pH=7	pH=0
△G0	0	0	0
△G1	-0.19441	-0.19441	-0.19441
△G2	0.10049	-0.72751	-1.55551
△G3	0.94112	0.11312	-0.71488
△G4	1.54973	0.72173	-0.10627
△G5	-0.60074	-1.01474	-1.42874
△G6	0.05332	-0.36068	-0.77468
△G7	-0.41218	-0.82618	-1.24018
△G8	-0.38926	-0.38926	-0.38926

Table S8. Calculated Gibbs free energies of Ag-Cu-P at different pH.

△G	pH=14	pH=7	pH=0
△G0	0	0	0
△G1	-0.50545	-0.50545	-0.50545
△G2	0.02979	-0.79821	-1.62621
△G3	0.49182	-0.33618	-1.16418
△G4	0.8757	0.0477	-0.7803
△G5	-0.26603	-0.68003	-1.09403
△G6	0.4082	-0.0058	-0.4198
△G7	0.3754	-0.0386	-0.4526
△G8	-0.36136	-0.36136	-0.36136

Table S9. The performance comparison of different electrocatalysts in alkaline electrolytes.

Catalyst	Electrolyte	Faraday efficiency (%)	Yield rate (μmol h/cm^2)	reference
Cu/Cu_2O nanowire	200 ppm+0.5 M Na_2SO_4	81.2	244.9	1
$NiCo_2O_4$/CP	0.1 M NaOH+0.1 M KNO_3	95.2	57.24	2
MP-Cu	1 M KOH+0.05 M NO_3^-	97.80	543	3
$Cu_{50}Ni_{50}$ alloy	1 M KOH+0.1 M KNO_3	93	416	4
Cu/TiO_2-	200 ppm NO_3^-	81.34	114.3	5
Fe SA	0.1 M K_2SO_4+0.5 M KNO_3	0.75	460	6
BCN@Cu	0.1 M KOH +100 mM KNO_3	89.3	348.48	7
Fe/Ni_2P	0.2 M K_2SO_4 +50 mM KNO_3	94.3	245	8
CoO_x	1 M NaOH +0.1 M $NaNO_3$	93.4	172.4	9
Co-SACs	1 M $NaNO_3$ +1 M NaOH	92	30.92	10
$Pt_{0.9}$/$Ce_{0.5}$-SS	0.1 M KNO_3 +0.5 M Na_2SO_4	94.12	599	11
Co/CoONSAs	14.33 mM NO_3^- +0.1 M Na_2SO^4	93.8	190	12
Fe single atom	0.5 M KNO_3 +0.1 M K_2SO_4	75	460	13
Cu-PTCDA	36 mM KNO_3 +0.1 M PBS	85.9	51.5	14
Ag-Cu-P	0.1 M KNO_3 + 1 MKOH	93.7	566.30	This work

Reference

(1) Wang, Y.; Zhou, W.; Jia, R.; Yu, Y.; Zhang, B. Unveiling the Activity Origin of a Copper-Based Electrocatalyst for Selective Nitrate Reduction to Ammonia. *Angew. Chem.-Int. Ed.* **2020**, *59* (13), 5350–5354. https://doi.org/10.1002/anie.201915992.

(2) Liu, Q.; Xie, L.; Liang, J.; Ren, Y.; Wang, Y.; Zhang, L.; Yue, L.; Li, T.; Luo, Y.; Li, N.; Tang, B.; Liu, Y.; Gao, S.; Alshehri, A. A.; Shakir, I.; Agboola, P. O.; Kong, Q.; Wang, Q.; Ma, D.; Sun, X. Ambient Ammonia Synthesis via Electrochemical Reduction of Nitrate Enabled by NiCo2O4 Nanowire Array. *SMALL* **2022**, *18* (13). https://doi.org/10.1002/smll.202106961.

(3) Wen, W.; Yan, P.; Sun, W.; Zhou, Y.; Yu, X.-Y. Metastable Phase Cu with Optimized Local Electronic State for Efficient Electrocatalytic Production of Ammonia from Nitrate. *Adv. Funct. Mater.* **2023**, *33* (6). https://doi.org/10.1002/adfm.202212236.

(4) Wang, Y.; Xu, A.; Wang, Z.; Huang, L.; Li, J.; Li, F.; Wicks, J.; Luo, M.; Nam, D.-H.; Tan, C.-S.; Ding, Y.; Wu, J.; Lum, Y.; Cao-Thang Dinh; Sinton, D.; Zheng, G.; Sargent, E. H. Enhanced Nitrate-to-Ammonia Activity on Copper-Nickel Alloys via Tuning of Intermediate Adsorption. *J. Am. Chem. Soc.* **2020**, *142* (12), 5702–5708. https://doi.org/10.1021/jacs.9b13347.

(5) Zhang, X.; Wang, C.; Guo, Y.; Zhang, B.; Wang, Y.; Yu, Y. Cu Clusters/TiO2-x with Abundant Oxygen Vacancies for Enhanced Electrocatalytic Nitrate Reduction to Ammonia. *J. Mater. Chem. A* **2022**, *10* (12), 6448–6453. https://doi.org/10.1039/d2ta00661h.

(6) Wu, Z.-Y.; Karamad, M.; Yong, X.; Huang, Q.; Cullen, D. A.; Zhu, P.; Xia, C.; Xiao, Q.; Shakouri, M.; Chen, F.-Y.; (Timothy) Kim, J. Y.; Xia, Y.; Heck, K.; Hu, Y.; Wong, M. S.; Li, Q.; Gates, I.; Siahrostami, S.; Wang, H. Electrochemical Ammonia Synthesis via Nitrate Reduction on Fe Single Atom Catalyst. *Nat. Commun.* **2021**, *12* (1). https://doi.org/10.1038/s41467-021-23115-x.

(7) Zhao, X.; Hu, G.; Tan, F.; Zhang, S.; Wang, X.; Hu, X.; Kuklin, A. V.; Baryshnikov, G. V.; Agren, H.; Zhou, X.; Zhang, H. Copper Confined in Vesicle-like BCN Cavities Promotes Electrochemical Reduction of Nitrate to Ammonia in Water. *J. Mater. Chem. A* **2021**, *9* (41), 23675–23686. https://doi.org/10.1039/d1ta05718a.

(8) Zhang, R.; Guo, Y.; Zhang, S.; Chen, D.; Zhao, Y.; Huang, Z.; Ma, L.; Li, P.; Yang, Q.; Liang, G.; Zhi, C. Efficient Ammonia Electrosynthesis and Energy Conversion through a Zn-Nitrate Battery by Iron Doping Engineered Nickel Phosphide Catalyst. *Adv. ENERGY Mater.* **2022**, *12* (13). https://doi.org/10.1002/aenm.202103872.

(9) Wang, J.; Cai, C.; Wang, Y.; Yang, X.; Wu, D.; Zhu, Y.; Li, M.; Gu, M.; Shao, M. Electrocatalytic Reduction of Nitrate to Ammonia on Low-Cost Ultrathin CoOx Nanosheets. *ACS Catal.* **2021**, *11* (24), 15135–15140. https://doi.org/10.1021/acscatal.1c03918.

(10) Li, J.; Li, M.; An, N.; Zhang, S.; Song, Q.; Yang, Y.; Li, J.; Liu, X. Boosted Ammonium Production by Single Cobalt Atom Catalysts with High Faradic Efficiencies. *Proc. Natl. Acad. Sci. U. S. A.* **2022**, *119* (29). https://doi.org/10.1073/pnas.2123450119.

(11) Chen, D.; Zhang, S.; Yin, D.; Li, W.; Bu, X.; Quan, Q.; Lai, Z.; Wang, W.; Meng, Y.; Liu, C.; Yip, S.; Chen, F.-R.; Zhi, C.; Ho, J. C. Tailored P-Orbital Delocalization by Diatomic Pt-Ce Induced Interlayer Spacing Engineering for Highly-Efficient Ammonia Electrosynthesis. *Adv. Energy Mater.* **2023**, *13* (6), 2203201. https://doi.org/10.1002/aenm.202203201.

(12) Yu, Y.; Wang, C.; Yu, Y.; Wang, Y.; Zhang, B. Promoting Selective Electroreduction of Nitrates to Ammonia over Electron-Deficient Co Modulated by Rectifying Schottky Contacts. *Sci. CHINA-Chem.* **2020**, *63* (10), 1469–1476. https://doi.org/10.1007/s11426-020-9795-x.

(13) Zhang, S.; Wu, J.; Zheng, M.; Jin, X.; Shen, Z.; Li, Z.; Wang, Y.; Wang, Q.; Wang, X.; Wei, H.; Zhang, J.; Wang, P.; Zhang, S.; Yu, L.; Dong, L.; Zhu, Q.; Zhang, H.; Lu, J. Fe/Cu Diatomic Catalysts for Electrochemical Nitrate Reduction to Ammonia. *Nat. Commun.* **2023**, *14* (1), 3634–3634. https://doi.org/10.1038/s41467-023-39366-9.

(14) Chen, G.-F.; Yuan, Y.; Jiang, H.; Ren, S.-Y.; Ding, L.-X.; Ma, L.; Wu, T.; Lu, J.; Wang, H. Electrochemical Reduction of Nitrate to Ammonia via Direct Eight-Electron Transfer Using a Copper-Molecular Solid Catalyst. *Nat. ENERGY* **2020**, *5* (8), 605–613. https://doi.org/10.1038/s41560-020-0654-1.